

Dual-Polarized Magnetic-Current Array Antennas with High Gain and Low Profile

Yue Li

Department of Electronic Engineering
Tsinghua University
Beijing 100084, China (CIE)
E-mail: lyee@tsinghua.edu.cn

Abstract

Two sets of feeding networks are usually needed to achieve a dual-polarized high-gain planar antenna, not only leading to a complicated configuration but also to reduced efficiency. A simple feed structure and strategy are therefore in high demand for dual-polarized high-gain planar antennas. Directed at this requirement, we first present a series-fed dual-polarized slot array with a single-layered substrate. Two orthogonal magnetic-current arrays were positioned at the opposite sides of a single-layered substrate, leading to high gain and high port isolation. A novel scheme to achieve dual-polarized, high-gain, and low-profile antennas using the higher-order-mode microstrip antenna was then demonstrated. By loading half-wavelength slots at the electric-field nulls of a higher-order-mode microstrip antenna, a multiple-element in-phase magnetic-current array was constructed within a low-profile cavity with a simple feeding strategy. As a proof of the concept, two dual-polarized high-gain microstrip magnetic-current array antennas, utilizing the TM_{50} and TM_{90} modes of a microstrip antenna were investigated. These magnetic-current array antennas had the merits of having a low profile, simple feeding, and high isolation, promising a huge potential in diversity and MIMO applications.

1. Introduction

Fifth-generation (5G) communication has raised increasing demands on the capacity, reliability, and spectrum efficiency of wireless-communication systems [1-3]. Under this scenario, antennas with dual-polarized operation are drawing great interest, because of their capability to boost the data transmission rate and to better resist multipath fading via polarization diversity [4]. Different types of dual-polarized antennas have been reported in the literature, including crossed dipoles [5-7], magneto-electric dipoles [8-10], slot antennas [11, 12], and microstrip antennas [13-17]. The key point to designing a dual-polarized antenna lies in keeping high isolation between the two excitation ports, which benefits the polarization purity. Another aspect favored by modern antenna systems is

high-gain performance that can be employed to compensate for path loss and add coverage range [17-22]. An antenna with high directivity can also be employed in satellite-to-ground communications [23, 24] and radar systems [25]. Furthermore, in the emerging technique of massive MIMO, a high-gain antenna array or lens serves the purpose of directing the beam to different sectors [26].

Nevertheless, there still remain great challenges in realizing high-gain antennas with dual-polarization operation. To a large extent, this stems from the high insertion loss and prohibitive cost of the complex feeding networks. Additionally, traditional schemes for arranging the radiating apertures and feeding lines at different layers [27-30] inevitably yield high profiles and inconvenience for integration with planar circuits. To address these thorny problems, we suggest a new scheme [31-33]: magnetic-current arrays, which offer dual-polarized and high-gain performance on single-layer substrates. In previous work [32], two orthogonally placed E-shaped slot arrays were series fed by coplanar waveguides connected to the same ground, while in [33] and [34] the high-order mode of a thin cavity was employed to excite the in-phase radiation of a magnetic-current array. Decent isolation levels between two polarizations were realized via the proper arrangement of radiating elements or feed lines. With compact structures and robust performance, the proposed magnetic-current arrays may open a new horizon for dual-polarized and high-gain antennas deployed in high-speed reliable wireless communications.

2. Dual-Polarized Magnetic-Current Array Antenna Using Series-Fed Slot Array

In this section, a dual-polarized slot antenna array etched on only a single layer of substrate is described, capable of being two-dimensionally scaled [32]. The geometry of this array is shown in Figure 1a. Two identical single-polarized slot arrays were arranged orthogonally on two sides of the substrate layer, which are represented in the figure by two different colors. Each row of elements on the

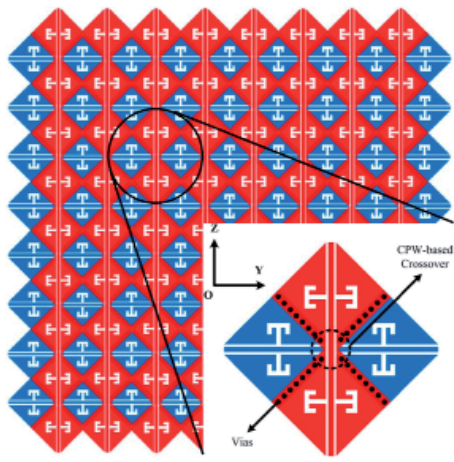


Figure 1a. A single-layer two-dimensional scalable dual-polarized series-fed slot array: the geometry and detailed view of the proposed array.

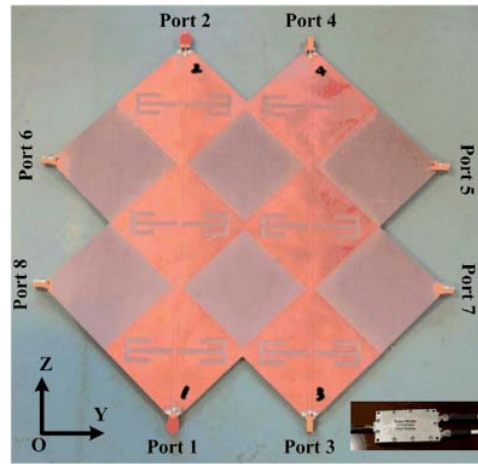


Figure 1b. A single-layer two-dimensional scalable dual-polarized series-fed slot array: a photograph of the proposed array.

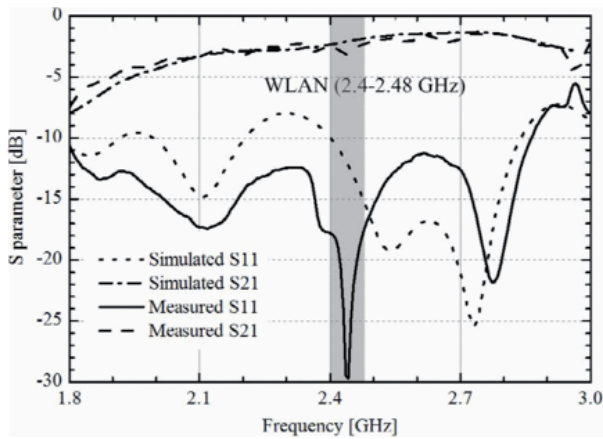


Figure 1c. A single-layer two-dimensional scalable dual-polarized series-fed slot array: the simulated and measured S parameters of the proposed array.

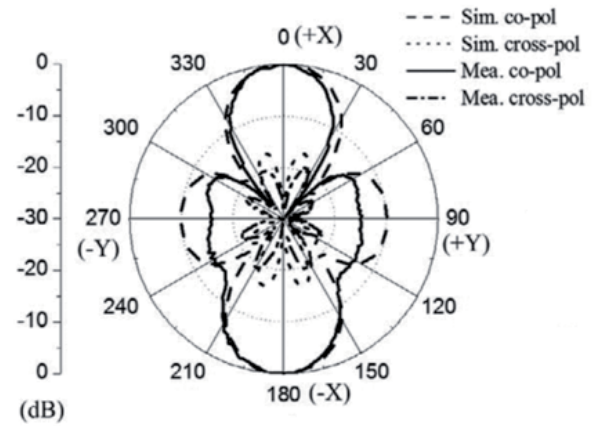


Figure 1d. A single-layer two-dimensional scalable dual-polarized series-fed slot array: the simulated and measured normalized radiation pattern at 2.4 GHz.

horizontal polarized slot array was series-fed by coplanar waveguide (CPW), and all the rows were excited by the power divider. Perpendicularly, the vertical polarized array was also series-fed using the same method. The unit cell of the whole slot array is shown in the detail view of Figure 1a. It was composed of slot elements, coplanar waveguide feeds, and a coplanar waveguide-based crossover. The half-wavelength slot element was grooved on the outer conductor of the coplanar waveguide, which was designed as an H-shaped slot due to size restrictions. Two adjacent slot elements on the one side were at a distance of one guided wavelength at 2.4 GHz. All elements could thus be excited in-phase at 2.4 GHz, so that each group of slot elements operated as a standing-wave array. This design eliminated the open stop band and rejected the absorbing loads at the end. At the intersection of two color areas, that is, the front and back sides of the unit cell, four lines of vias were designed to connect two sides of the substrate board and to make all the slots equipotential. By using the

vias and the coplanar-waveguide-based crossover, the unit cell achieved lower reflection coefficient (S_{11}), higher transmission coefficient (S_{21}), and better port isolation (S_{31} and S_{41}).

To prove the proposed structure as shown in Figure 1b, a 12-element slot array with a 3×2 element array for each polarization was processed and measured. Figure 1c shows the simulated and measured S parameters of the proposed array, where Port 1 was excited and the other ports were loaded. In the WLAN band, a reflection coefficient lower than -18 dB was achieved, with a transmission coefficient from -2.6 dB to -3.2 dB. Apart from this, the isolation of all of the ports was lower than -20 dB in the frequency band of 2.4 GHz to 2.48 GHz. To excite the proposed array, a 1-to-2 divider was used to feed through Port 1 and Port 3. The simulated and measured normalized radiation patterns in the xoy -plane at 2.4 GHz are shown in Figure 1d, in which bidirectional patterns were obtained with a sidelobe level

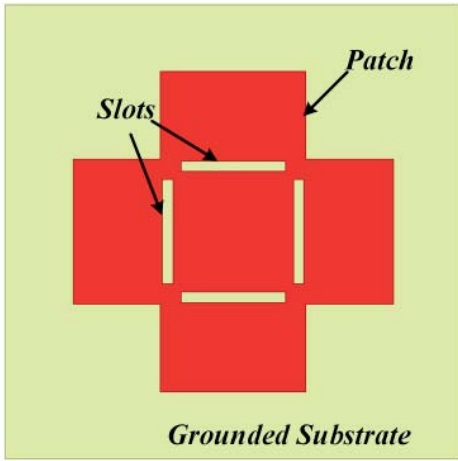


Figure 2a. The proposed dual-polarized, high-gain, and low-profile microstrip antenna based on the hybridized higher-order TM_{50} mode: a top view of the structure and the geometry.

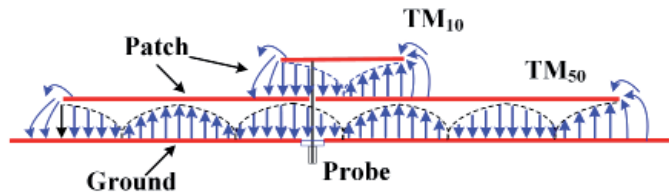


Figure 2b. A sketch of sectional electric vector field distribution of the dual-mode stacked microstrip antenna as in [31] for the antenna in Figure 2a.

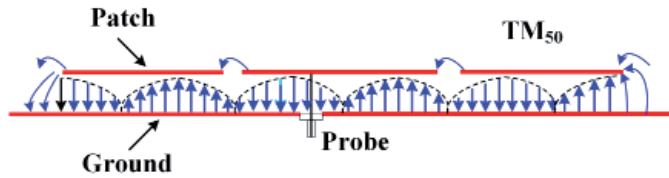


Figure 2c. A sketch of the electric vector field distribution of the proposed antenna shown in Figure 2a.

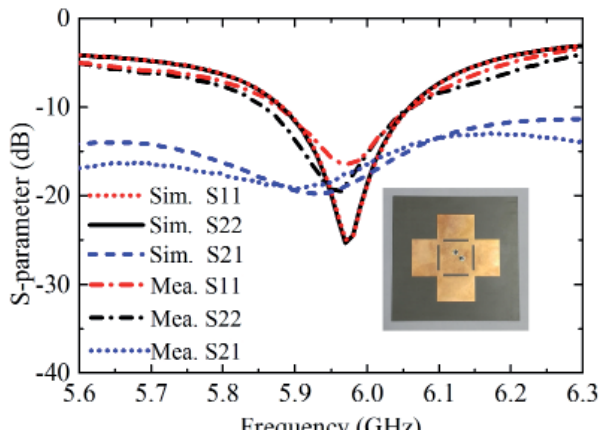


Figure 2d. The fabricated prototype and measured S parameters for the antenna in Figure 2a.

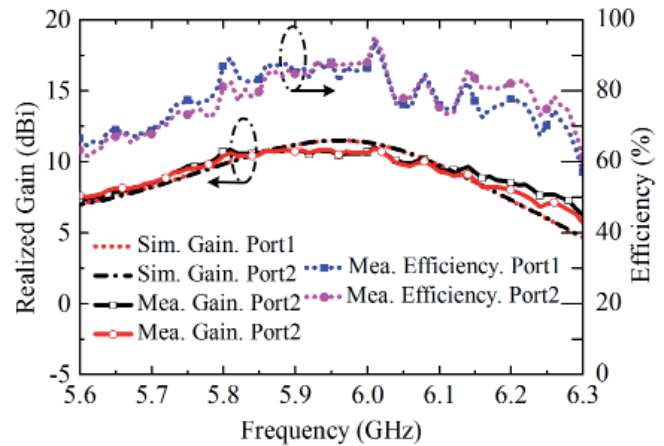


Figure 2e. The simulated and measured efficiency and gain of the two feeding ports for the antenna in Figure 2a.

lower than -10 dB. The radiation efficiency was 97.7% that getting rid of the mismatch, which could be reduced using a matching network. Compared with the structure of a conventional of dual-polarized array, this design used only one substrate board and coplanar-waveguide-based crossovers for compact construction, and can be two-dimensionally expanded without additional complexity.

3. Dual-Polarized Magnetic-Current Antenna Using the TM_{50} -Mode Microstrip Antenna

In this section, a higher-order TM_{50} mode was excited to obtain a dual-polarized microstrip antenna with significant gain enhancement [33], especially when compared with those conventional microstrip antennas operating at the TM_{10} mode. The geometry of this antenna is shown

in Figure 2a. It was composed of a pair of orthogonal patches, four etched slots, and a single-layer grounded substrate. The operating principle is described through Figures 2b-2c. Because the dual-polarized antenna had a symmetric structure, only the polarization along the y -axis was analyzed as an example. Starting from a hybrid-mode single-polarized stacked microstrip antenna, inspired from the design concept in [31], the side view and a sketch of the sectional electric vector field distribution are shown in Figure 2b. The lower patch operated in the TM_{50} mode, and the upper suspended patch operated in the TM_{10} mode. It can be seen from the E-field distribution that the radiating edges of the two patches had in-phase superposition, which resulted in gain enhancement in the broadside direction. To modify the dual-layer structure into a single-layer structure, as shown in Figure 2c, two slots were etched on the lower patch to replace two radiating magnetic-currents of the upper patch, and a four-element in-phase single-polarized magnetic-current array was achieved. In the proposed

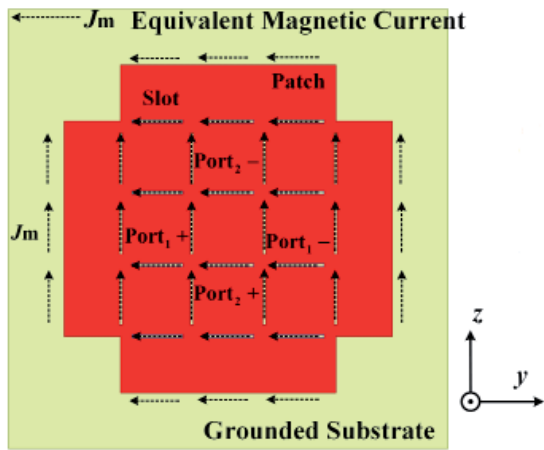


Figure 3a The proposed dual-polarized, high-gain, and low-profile magnetic-current array antenna based on a TM_{90} -mode microstrip antenna: the general structure and working principles.

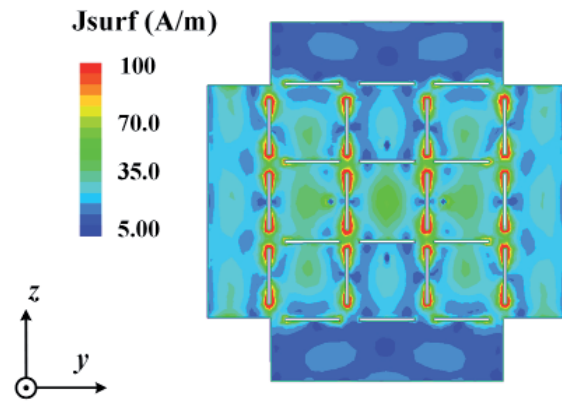


Figure 3b. The amplitude of the surface-current distribution for the antenna in Figure 3a.

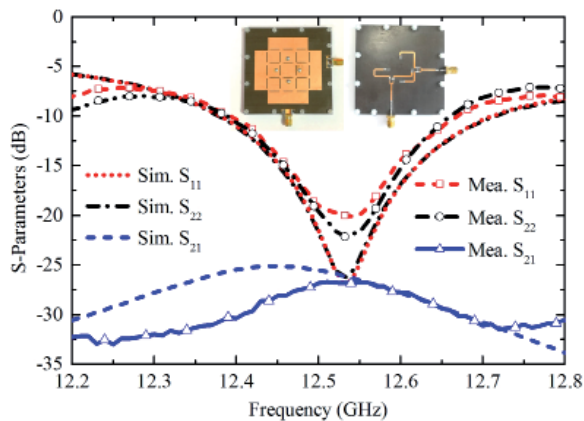


Figure 3c. The fabricated prototype and the measured and simulated S parameters for the antenna in Figure 3a.

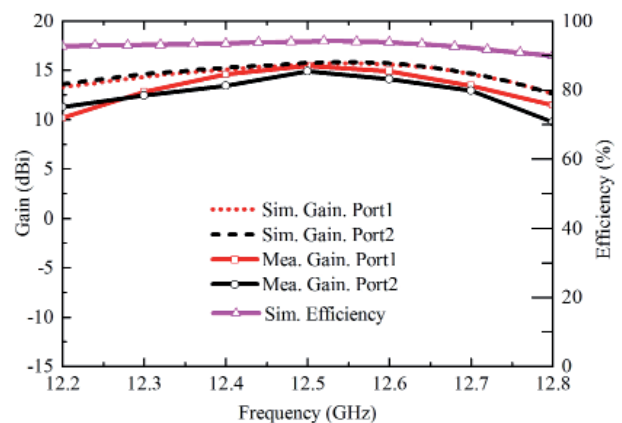


Figure 3d. The measured and simulated gains and efficiencies for the antenna in Figure 3a.

structure, a higher broadside gain was therefore realized by combining the radiating fields of two slots and the TM_{50} -mode patch. The polarization along the z axis operated under the same mechanism, and the dual-polarized antenna was easily constructed by combining these two polarizations.

The proposed antenna was fabricated. Its top view is shown in the inset of Figure 2, which also presents the simulated and measured S parameters. Two polarizations both achieved a -10 dB bandwidth of 5.88 GHz to 6.06 GHz, and obtain a good isolation of less than -14 dB. As shown in Figure 2, it was observed that the measured peak broadside gain of this antenna was 10.9 dBi, which is much higher than that of conventional microstrip antennas. Providing the merits of dual polarization, high broadside gain, simple feeding, and a single-layer structure, the proposed microstrip antenna using the slot-loaded TM_{50} mode has obvious potential applications in MIMO and 5G communication systems.

4. Dual-Polarized Magnetic-Current Array Using the TM_{90} -Mode Microstrip Antenna

In this section, a dual-polarized high-gain microstrip magnetic-current array antenna based on the higher-order TM_{90} mode is described [34]. Figure 3 shows the structure of the proposed dual-polarized high-gain antenna fed by two simple orthogonal differential ports. As can be seen in Figure 3a, $3 \times 4 \times 2$ slots were located at the maximum point of the current on a patch antenna operating with the TM_{90} mode to achieve an in-phase 3×6 magnetic-current array for single-polarized high-gain radiation. By rotating the slotted patch 90° and combining together these two antennas, a dual-polarized high-gain antenna could be constructed. The antenna was fed by a simple feeding network with two differential pairs. Each pair contained a Wilkinson power divider and a microstrip delay line to generate two anti-phase excitations. The operating principle could be explained

through the current distribution shown in Figure 3b. Fed by port 1, the patch was excited at its TM_{90} mode. At the edges of the patch were the maximums of the electric fields, and two equivalent magnetic currents were formed. 3×4 slots, each of a half wavelength, were located perpendicular to the current at the nulls of electric fields, producing an additional 12 magnetic currents. A 3×6 magnetic-current array could therefore be excited by port 1, which was also compliant with the vertical feeding situations.

A prototype of the antenna was fabricated and measured. A photo of this prototype and the measured S parameters are depicted in Figure 3c, which shows agreement with simulated results. The impedance bandwidths of the two polarizations were from 12.38 GHz to 12.72 GHz. The gain and efficiency of the antenna is shown in Figure 3d. The maximum gain was 15.5 dBi at 12.52 GHz, and the radiation efficiency was above 90% over the operating bands.

5. Conclusion

In this paper, two different kinds of dual-polarized high-gain low-profile magnetic-current array antennas with a simple feeding strategy have been presented. For the first kind, by positioning two sets of coplanar waveguide-fed slot arrays orthogonally on opposite sides of a single substrate, a $2 \times 3 \times 2$ -element dual-polarized magnetic-current array was achieved with the merits of two-dimensional scalability, a simple feed, a single substrate layer, and high isolation. For the second kind, by loading half-wavelength slots on the electric-field nulls of a higher-order-mode microstrip antenna, a multiple-element in-phase magnetic-current array could be formed within a low-profile cavity with a simple feed and high isolation. As a validation for the proposed method, a dual-polarized 2×4 -element in-phase magnetic-current array operating at 5.8 GHz was then designed using a TM_{50} -mode microstrip antenna, with the merits of a single feed, a single-layered configuration, and high isolation. The maximum gain reached 10.9 dBi within a compact volume of $1.65 \lambda_0 \times 1.65 \lambda_0 \times 0.04 \lambda_0$. Last but not least, a dual-polarized 36-element ($3 \times 6 \times 2$) magnetic-current array antenna with a simple differential feed was experimentally implemented within a total size of $2.92 \lambda_0 \times 2.92 \lambda_0 \times 0.085 \lambda_0$. This antenna achieved high isolation – better than 25 dB – and a maximum gain of 15.5 dBi within an operating bandwidth of 12.39 GHz to 12.68 GHz. In summary, these proposed antennas have the advantages of a low profile, a simple feed, and high isolation, exhibiting promising applications in diversity and MIMO systems, and in 5G communications.

6. References

1. M. A. Jensen and J. W. Wallace, "A review of antennas and propagation for MIMO wireless communication," *IEEE Trans. Antennas Propag.*, **52**, 11, 2004, pp. 2810-2824.
2. P. S. Kildal and K. Rosengran, "Correlation and capacity of MIMO systems and mutual coupling, radiation efficiency, and diversity gain of their antennas: Simulations and measurements in a reverberation chamber," *IEEE Commun. Mag.*, **42**, 12, 2004, pp. 102-112.
3. S. C. K. Ko and R. D. Murch, "Compact integration diversity antenna for wireless communications," *IEEE Trans. Antennas Propag.*, **49**, 6, 2001, pp. 954-960.
4. R. G. Vaughan, "Polarization diversity in mobile communications," *IEEE Trans. Veh. Technol.*, **39**, 3, 1990, pp. 177-186.
5. K. Mak, H. Wong, and K. Luk, "A shorted bowtie patch antenna with a cross dipole for dual polarization," *IEEE Antennas Wireless Propag. Lett.*, **6**, 2007, pp. 126-129.
6. Y. Gou, S. Yang, J. Li, and Z. Nie, "A compact dual-polarized printed dipole antenna with high isolation for wideband base station applications," *IEEE Trans. Antennas Propag.*, **62**, 8, 2014, pp. 4392-4395.
7. Y. Cui, X. Gao, H. Fu, Q.-X. Chu, and R. Li, "Broadband dual-polarized dual-dipole planar antennas: Analysis, design, and application for base stations," *IEEE Antennas Propag. Mag.*, **59**, 6, 2017, pp. 77-87.
8. Q. Xue, S. Liao, and J. Xu, "A differentially-driven dual-polarized magneto-electric dipole antenna," *IEEE Trans. Antennas Propag.*, **61**, 1, 2013, pp. 425-430.
9. Q. Wu and K. M. Luk, "A broadband dual-polarized magnetolectric dipole antenna with simple feeds," *IEEE Antennas Wireless Propag. Lett.*, **8**, 2009, pp. 60-63.
10. S. G. Zhou, Z. H. Peng, G. L. Huang, and C. Y. Sim, "Design of a novel wideband and dual polarized magnetolectric dipole antenna," *IEEE Trans. Antennas Propag.*, **65**, 5, 2017, pp. 2645-2649.
11. Y. Li, Z. J. Zhang, J. F. Zheng, and Z. H. Feng, "Compact azimuthal omnidirectional dual-polarized antenna using highly isolated collocated slots," *IEEE Trans. Antennas Propag.*, vol. **60**, 9, 2012, pp. 4037-4045.
12. Y. Li, Z. Zhang, W. Chen, Z. Feng, and M. F. Iskander, "A dual-polarization slot antenna using a compact CPW feeding structure," *IEEE Antennas Wireless Propag. Lett.*, **9**, 2010, pp. 191-194.
13. K. D. M. Pozar and D. H. Schaubert, *Microstrip Antennas: The Analysis and Design of Microstrip Antennas and Arrays*, New York, USA, IEEE Press, 1995.
14. Q. Li, S. W. Cheung, and C. Zhou, "A low-profile dual-polarized patch antenna with stable radiation pattern using ground-slot groups and metallic ground wall," *IEEE Trans. Antennas Propag.*, **65**, 10, October 2017, pp. 5061-5068.

15. X. Zhang and L. Zhu, "Gain-enhanced patch antennas with loading of shorting pins," *IEEE Trans. Antennas Propag.*, **64**, 8, August, 2016, pp. 3310-3318.
16. D. Sun, Z. Zhang, X. Yan, and X. Jiang, "Design of broadband dual polarized patch antenna with backed square annular cavity," *IEEE Trans. Antennas Propag.*, **64**, 1, January 2016, pp. 43-52.
17. Z. Tang, J. Liu, Y.-M. Cai, J. Wang, and Y. Yin, "A wideband differentially fed dual-polarized stacked patch antenna with tuned slot excitations," *IEEE Trans. Antennas Propag.*, **66**, 4, April 2018, pp. 2055-2060.
18. P. S. Hall and C. M. Hall, "Coplanar corporate feed effects in microstrip patch array design," *IEE Proc. H-Microw., Antennas Propag.*, **135**, 3, 1988, pp. 180-186.
19. J. Huang, "A Ka-band circularly polarized high-gain microstrip array antenna," *IEEE Trans. Antennas Propag.*, **43**, 1, January 1995, pp. 113-116.
20. H. D. Chen, C. Y. D. Sim, J. Y. Wu, and T. W. Chiu, "Broadband high gain microstrip array antennas for WiMAX base station," *IEEE Trans. Antennas Propag.*, **60**, 8, August 2012, pp. 3977-3980.
21. Y. Wang and Z. Du, "Dual-polarized slot-coupled microstrip antenna array with stable active element pattern," *IEEE Trans. Antennas Propag.*, **63**, 9, September 2015, pp. 4239-4244.
22. R. Lian, Z. Wang, Y. Yin, J. Wu, and X. Song, "Design of a low profile dual-polarized stepped slot antenna array for base station," *IEEE Antennas Wireless Propag. Lett.*, **15**, 2016, pp. 362-365.
23. E. Arneri, L. Boccia, G. Amendola and G. Di Massa, "A Compact High Gain Antenna for Small Satellite Applications," *IEEE Transactions on Antennas and Propagation*, **55**, 2, February 2007, pp. 277-282.
24. W. Hong et al., "Multibeam Antenna Technologies for 5G Wireless Communications," *IEEE Transactions on Antennas and Propagation*, **65**, 12, December 2017, pp. 6231-6249.
25. M. I. Skolnik, *Introduction to Radar Systems*, New York, NY, USA, McGraw-Hill, 1980.
26. E. Rammos, "New wideband high-gain stripline planar array for 12 GHz satellite TV," *Electronics Letters*, **18**, 6, March 1982, pp. 252-253.
27. D. Pozar and S. Targonski, "A shared-aperture dual-band dual-polarized microstrip array," *IEEE Trans. Antennas Propag.*, **49**, 2, February 2001, pp. 150-157.
28. H. Wong, K. G. Lau, and K. Luk, "Design of dual-polarized L-probe patch antenna arrays with high isolation," *IEEE Trans. Antennas Propag.*, **52**, 1, January 2004, pp. 45-52.
29. S. Gao and A. Sambell, "Low-cost dual-polarized printed array with broad bandwidth," *IEEE Trans. Antennas Propag.*, **52**, 12, December 2004, pp. 3394-3397.
30. G. Vetharatnam, C. Kuan, and C. Teik, "Combined feed network for a shared-aperture dual-band dual-polarized array," *IEEE Antennas Wireless Propag. Lett.*, **4**, 2005, pp. 297-299.
31. P. Juyal and L. Shafai, "A high gain single feed dual mode microstrip disc radiator," *IEEE Trans. Antennas Propag.*, vol. 64, 6, June 2016, pp. 2115-2126.
32. Y. Li, Z. Zhang, C. Deng, Z. Feng and M. F. Iskander, "2-D Planar Scalable Dual-Polarized Series-Fed Slot Antenna Array Using Single Substrate," *IEEE Trans. Antennas Propag.*, **62**, 4, April 2014, pp. 2280-2283.
33. Y. He, Y. Li, W. Sun, Z. Zhang and P. Chen, "Dual Linearly Polarized Microstrip Antenna Using a Slot-Loaded TM_{50} Mode," *IEEE Antennas Wireless Propag. Lett.*, **17**, 12, December 2018, pp. 2344-2348.
34. Y. He, Y. Li, W. Sun and Z. Zhang, "Dual-Polarized, High-Gain, and Low-Profile Magnetic Current Array Antenna," *IEEE Trans. Antennas Propag.*, **67**, 2, February 2019, pp. 1312-1317.